Polarity control of ZnO films on (0001) Al2O3 by Cr-compound intermediate layers

doi: 10.1063/1.2740190

Polarity control of ZnO films on (0001) Al_2O_3 by Cr-compound intermediate layers

J. S. Park[a)]
Institute for Materials Research, Tohoku University, Katahira 2-1-1, Aoba-ku, Sendai 980-8577, Japan

S. K. Hong
Department of Nano Information Systems Engineering, Chungnam National University, Daejeon 305-764, Korea

T. Minegishi, S. H. Park, I. H. Im, T. Hanada, M. W. Cho,[b)] and T. Yao[b)]
Institute for Materials Research, Tohoku University, Katahira 2-1-1, Aoba-ku, Sendai 980-8577, Japan

J. W. Lee and J. Y. Lee
Department of Materials Science and Engineering, Korea Advanced Institute of Science and Technology, Daejeon 305-701, Korea

(Received 2 February 2007; accepted 24 April 2007; published online 15 May 2007)

This letter presents a reliable and very easy method for selective growth of polarity controlled ZnO films on (0001) Al_2O_3 substrates by plasma-assisted molecular-beam epitaxy. Cr-compound intermediate layers are used to control the crystal polarity of ZnO films on (0001) Al_2O_3. ZnO films grown on rocksalt structure CrN/(0001) Al_2O_3 shows Zn polarity, while those grown on rhombohedral Cr_2O_3/(0001) Al_2O_3 shows O polarity. Possible interface atomic arrangements for both heterostructures are proposed. © *2007 American Institute of Physics*.
[DOI: 10.1063/1.2740190]

ZnO is an attractive material for applications to ultraviolet optoelectronic devices owing to its wide band gap of 3.37 eV and a large exciton binding energy of 60 meV at room temperature.[1] ZnO crystallizes in wurtzite structure and naturally has crystal polarity along the *c* axis: Zn polar and O polar. Chemical, optical, and electrical properties of ZnO are dependent on crystal polarity.[2–5] It has been reported that the efficiency for impurity doping in GaN (Ref. 6) and ZnO (Ref. 7) depends on crystal polarity. Polarity dependent doping will be important to achieve reliable *p*-type ZnO. Crystal polarity is one of the important factors for designing electronic and optoelectronic devices.[8,9] To date, only a few methods have been reported on the control of crystal polarity of ZnO films on *c* sapphire.[10,11] Selective growth of Zn- and O-polar ZnO layers were achieved on *c* sapphire by using thickness-controlled MgO buffer.[10] Ultrathin AlN buffer layers, which were formed by nitridation of the surface of *c* sapphire, were used to control the crystal polarity of ZnO layers grown on *c* sapphire.[11] We mention, however, that special precaution is needed to prepare the MgO and AlN buffers, which play a crucial role in the selective growth of Zn-polar and O-polar ZnO layers on *c* sapphire.

This letter will report on an easy and reliable method for selective growth of polarity-controlled ZnO films on (0001) Al_2O_3 substrates by plasma-assisted molecular-beam epitaxy. Cr-compound intermediate layers are used to control the crystal polarity of ZnO films on (0001) Al_2O_3. ZnO films grown on rocksalt structure CrN/(0001) Al_2O_3 shows Zn polarity, while those grown on rhombohedral Cr_2O_3/(0001) Al_2O_3 shows O polarity. Possible interface atomic arrangements for both heterostructures will be proposed.

CrN films were grown on *c* sapphire at 700 °C with metal Cr and ammonia as sources of Cr and N, respectively. Cr_2O_3 layers were formed through oxidation of CrN/*c* sapphire by exposing oxygen plasma at 650 °C for 10 min. The formation processes of Cr_2O_3 on CrN layers were monitored by *in situ* reflection high-energy electron diffraction (RHEED). ZnO films were grown at 700 °C with a Zn beam flux of 1.6 A/s, oxygen flow rate at 1 SCCM (denotes cubic centimeter per minute at STP), and an rf power of 300 W. In order to prevent oxidation of the surface of CrN layer,[12] Zn beam was exposed onto the CrN at 400 °C prior to ZnO growth.

The crystal structure and phase identification of each layer were investigated by the high-resolution transmission electron microscopy (HRTEM). The crystal polarity of ZnO layers was determined based on differences in etching rate and growth rate between Zn-polar ZnO and O-polar ZnO. For etching-rate measurements, chemical wet etching was carried out using 0.01 *M* hydrochloric acid solution at room temperature. Changes in the surface morphology of ZnO by wet etching were also assessed by atomic force microscopy (AFM).

Figure 1 shows the cross-sectional HRTEM micrograph for a ZnO film grown on a CrN/Al_2O_3 substrate. Digital diffraction patterns (DDPs) obtained by fast Fourier transformation (FFT) of the HRTEM image are also shown in the figure. The DDPs are obtained from the marked square regions on the HRTEM image. The corresponding DDPs from ZnO and Al_2O_3 reveal typical diffraction patterns of ZnO and Al_2O_3 for the $\langle 11-20 \rangle$ and $\langle 10-10 \rangle$ zone axes, respectively. Based on the camera constant determined from the DDPs for ZnO and Al_2O_3, the DDP from the intermediate layer is indexed and determined to be the diffraction pattern for the rocksalt structure CrN with the $\langle 110 \rangle$ zone axis. The CrN layer is single crystalline with a thickness of 2.5 nm. Here, it should be noted that there

[a)]Author to whom correspondence should be addressed; electronic mail: jspark@imr.tohoku.ac.jp
[b)]Also at: Center for Interdisciplinary Research, Tohoku University, Sendai 980-8578, Japan.

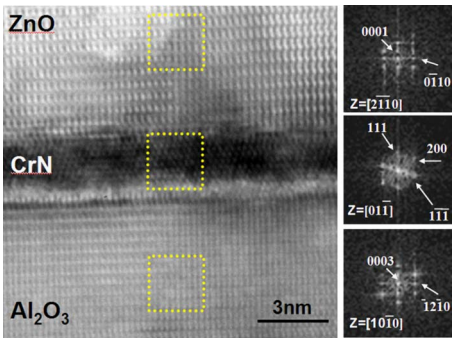

FIG. 1. (Color online) Cross-sectional HRTEM micrograph of the $ZnO/CrN/Al_2O_3$. DDPs for the ZnO, CrN, and Al_2O_3 are shown in the right, which are obtained by the FFT of the marked square regions of the image.

is no additional oxide interfacial layer between the ZnO and CrN, which means that the oxidation of the CrN layer was protected by the Zn preexposure before the growth of the ZnO.[12] From the TEM study, we have determined the epitaxial relationship between the ZnO, CrN, and Al_2O_3 as $ZnO(0001)\|CrN(111)\|Al_2O_3(0001)$ and $ZnO[2-1-10]\|CrN[01-1]\|Al_2O_3[10-10]$.

Figure 2 shows the cross-sectional HRTEM micrograph for a ZnO film grown on an oxidized CrN/Al_2O_3 substrate. We can clearly see two intermediate layers between the ZnO and Al_2O_3. The DDPs for the ZnO, Al_2O_3, and two intermediate layers are shown in the inset of Fig. 2. The lower intermediate layer is determined to be CrN based on the DDP analysis with the same procedures mentioned in Fig. 1. The DDP from the upper intermediate layer is indexed and determined to be a diffraction pattern for rhombohedral structure Cr_2O_3 with the $\langle 01-10\rangle$ zone axis. The Cr_2O_3 layer is single crystalline with a thickness of 3.5 nm. Therefore, we have concluded that the top CrN layer was oxidized and changed to a Cr_2O_3 layer, which was expected from a change in RHEED pattern during oxidation.[13] From the TEM and RHEED evolutions, the epitaxial relationship between the layers is determined to be as follows: $ZnO(0001)\|Cr_2O_3(0001)\|CrN(111)\|Al_2O_3(0001)$ and $ZnO[2-1-10]\|Cr_2O_3[10-10]\|CrN[01-1]\|Al_2O_3[10-10]$. In addition, we have measured x-ray diffraction

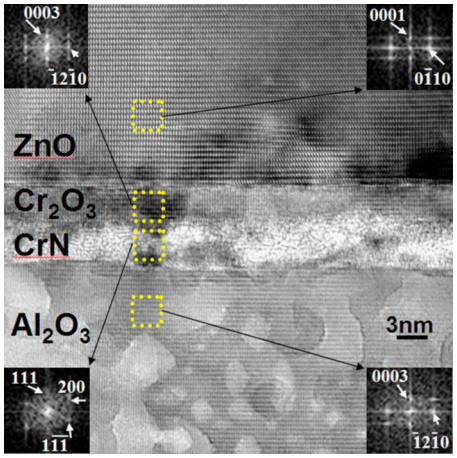

FIG. 2. (Color online) Cross-sectional HRTEM micrographs of $ZnO/Cr_2O_3/CrN/Al_2O_3$. DDPs for the ZnO, Cr_2O_3, CrN, and Al_2O_3 are shown in the insets, which are obtained by the FFT of the marked square regions of the image.

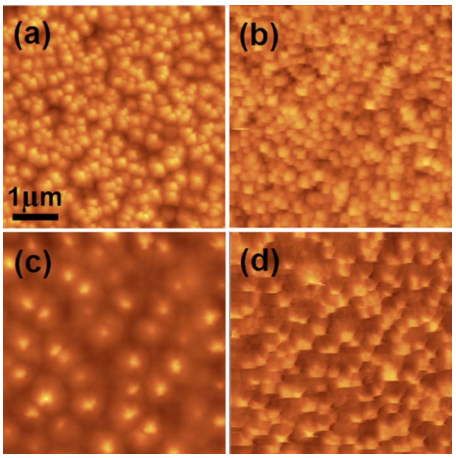

FIG. 3. (Color online) AFM images for the ZnO films before [(a) and (c)] and after [(b) and (d)] chemical etching on the CrN [(a) and (b)] and on the Cr_2O_3 [(c) and (d)].

(XRD) θ-2θ and Φ scans (not shown here). The XRD θ-2θ diffraction curve showed only the (0002) peak of ZnO indicating that the plane parallel to the interface is only (0002). In case of the XRD Φ scan of ZnO (10−11) planes, six peaks regularly spaced by 60° were observed, which indicates that there are no rotational domains.

Let us discuss the crystal polarity of the two kinds of ZnO films shown in Figs. 1 and 2. The polarity of ZnO films was determined by investigating differences in wet etching and growth rate. The difference in etching rate for opposite polar faces has been explained in terms of surface bonding model for A_{II}-B_{VI}.[14] The surface Zn layer has a positive charge, while the layer of surface O atoms has a negative charge with the two dangling electrons due to the electron transfer from Zn to O atoms.[15] The dangling electrons on O-polar surfaces account for a high etching rate, owing to their susceptibility to reaction with electron-seeking agents, than those on Zn-polar surfaces.[15] Hence, both wurtzite-structure III-nitrides[16–18] and ZnO (Refs. 19 and 20) show different etching rates for surfaces with different crystal polarities, which implies that the polarity determination based on a chemical etching rate is highly reliable. Chemical wet etching rates of ZnO films grown on CrN and Cr_2O_3/CrN layers were determined to be 10 and 95 nm/min, respectively; which reveals about ten times higher etching rate for the ZnO film grown on a Cr_2O_3/CrN layer. Such remarkable difference in wet etching rate clearly indicates that ZnO films grown on a CrN has Zn polarity, while the one grown on a Cr_2O_3/CrN has O polarity. Figures 3(a) and 3(b) show that the surface morphology of ZnO films grown on CrN layer is only slightly changed after chemical etching and that the rms value is only changed from 32.4 to 33.2 nm by chemical etching. To the contrary, the surface of ZnO films grown on Cr_2O_3/CrN become rough by chemical etching, as shown in Figs. 3(c) and 3(d). The rms value measures 16.9 and 52.8 nm before and after etching, respectively. All these observed surface features on our samples agree well with the etching characteristics of different polar ZnO films.[15,19,20] Therefore, we conclude that ZnO films grown on CrN are Zn polar, while ZnO films on Cr_2O_3/CrN are O polar.

It has been reported that the growth rate of Zn-polar ZnO is considerably higher than that of O-polar films.[19,21] The higher growth rate for Zn-polar ZnO films can be understood

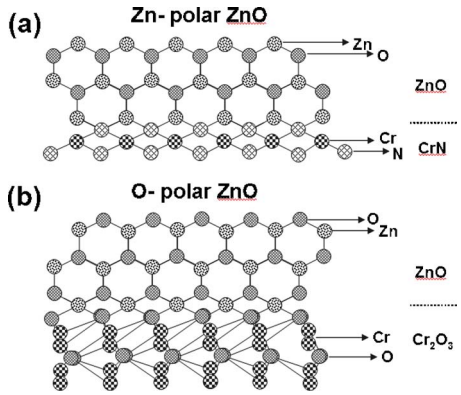

FIG. 4. (Color online) Schematics of the atomic arrangements of ZnO layers on CrN layer (a) and on Cr_2O_3 layer (b), which result in Zn-polar and O-polar ZnO, respectively.

in terms of the difference in the sticking coefficient of Zn atoms onto growing surfaces, since the growth of ZnO films is mostly limited by the sticking of Zn atoms rather than that of O atoms under O-rich growth conditions.[22] Each oxygen atom on a Zn-polar surface has three dangling bonds, while each O atom has only one dangling bond on an O-polar surface. Hence, the sticking coefficient of Zn atoms onto an O-terminated surface of Zn-polar ZnO is larger than that onto an O-polar ZnO, which results in a higher growth rate for Zn-polar ZnO films than that for O-polar ZnO films.[22] In our samples, the typical growth rate of ZnO films grown on CrN was 7.5 nm/min, while those grown on Cr_2O_3/CrN showed a growth rate of 4.9 nm/min under the same growth conditions. The growth rate of ZnO films grown on CrN layer is 1.5 times higher than that of ZnO films grown on Cr_2O_3/CrN layer. Hence, we can conclude that ZnO films grown on CrN are Zn polar, while those grown on Cr_2O_3/CrN are O polar. This conclusion is consistent with the etching studies described above.

Figures 4(a) and 4(b) show schematics of the atomic arrangements of ZnO on CrN and Cr_2O_3, respectively. The CrN surface is mostly N terminated because the CrN growth was conducted under N-rich growth conditions. In the initial growth of ZnO on CrN, we have employed Zn preexposure to prevent oxidation of the CrN, as mentioned before. Therefore, we expect N–Zn bondings at the interface. Since the topmost N atoms in rocksalt CrN have three dangling bonds, each Zn atom bonded with N atoms has only one dangling bond along the growth direction. O atoms bonding to Zn atoms have three dangling bonds. As a result, ZnO films grown on CrN layer shows Zn polarity, as shown in Fig. 4(a). When Cr_2O_3 is formed by the exposure of oxygen plasma, the topmost surface is likely to be an O-terminated surface based on the reported surface phase diagram.[23] Zn atoms at the interface will occupy octahedral sites bonding to three underlying oxygen atoms in the oxygen layer of Cr_2O_3 and will simultaneously occupy tetrahedral sites of ZnO as in the case of AlN formation on O-terminated (0001) Al_2O_3 by nitridation.[24] Therefore, every oxygen atom at the surface has one dangling bond along the *c* direction, which results in O-polar ZnO layers.

Finally, in order to demonstrate the crucial role of Cr_2O_3 intermediate layer in determining the polarity of ZnO grown on Al_2O_3 structure, we have checked the polarity of a ZnO film grown on Cr_2O_3 without underlying CrN layer.[25] ZnO films grown on the Cr_2O_3 showed the same growth rate as that of the ZnO film in Fig. 2, which indicates that O-polar ZnO films grow on Cr_2O_3 layer. Therefore, we can conclude that the key factors for the selective growth of Zn- and O-polar ZnO films on Al_2O_3 are the use of intermediate layers of CrN with cubic O sublattice and Cr_2O_3 with hexagonal O sublattice, respectively.

In summary, we have controlled the polarity of ZnO films grown on (0001) Al_2O_3 by using Cr-compound intermediate layers. Single crystalline ZnO films were grown on (111) CrN and (0001) Cr_2O_3 layers by PAMBE. Phases and crystal structures of the intermediate layers and epitaxial relationships were investigated by HRTEM. A very low chemical etching rate and a higher growth rate were observed for ZnO films grown on CrN layer, while a high chemical etching rate and a lower growth rate were observed for those grown on Cr_2O_3 layer. Based on these observations, the polarity of ZnO films grown on rocksalt structure CrN is determined to be Zn polar, while O-polar ZnO films are grown on rhombohedral Cr_2O_3 layer. Possible interface atomic arrangements for both heterostructures are proposed.

The CNU portion was supported by Korea Research Foundation Grant funded by Korea Government (MOEHRD, Basic Research Promotion Fund) (KRF-2005-205-D00078).

[1] D. M. Bagnall, Y. F. Chen, Z. Zhu, S. Koyama, M. Y. Shen, T. Goto, and T. Yao, Appl. Phys. Lett. **70**, 2230 (1997).
[2] H. Matsui, H. Saeki, T. Kawai, A. Sasaki, M. Yoshimoto, M. Tsubaki, and H. Tabata, J. Vac. Sci. Technol. B **22**, 2454 (2005).
[3] S. A. Chevtchenko, J. C. Moore, U. Ozgur, X. Gu, A. A. Baski, H. Morkoc, B. Nemeth, and J. E. Nause, Appl. Phys. Lett. **89**, 182111 (2006).
[4] S. K. Hong, T. Hanada, H. J. Ko, Y. Chen, D. Imai, K. Araki, M. Shinohara, K. Saitoh, M. Terauchi, and T. Yao, Phys. Rev. B **65**, 115331 (2002).
[5] M. Losurdo and M. M. Giangregorio, Appl. Phys. Lett. **86**, 091901 (2005).
[6] A. J. Ptak, Th. H. Myers, L. T. Romano, C. G. Van de Walle, and J. E. Northup, Appl. Phys. Lett. **78**, 285 (2001).
[7] K. Nakahara U.S. Patent No. 7,002,179 (4 February 2004).
[8] J. Cai and F. A. Ponce, J. Appl. Phys. **91**, 9856 (2002).
[9] H. Tampo, H. Shibat, K. Matsubara, A. Yamada, P. Fons, S. Niki, M. Yamagata, and H. Kanie, Appl. Phys. Lett. **89**, 132113 (2006).
[10] H. Kato, K. Miyamoto, M. Sano, and T. Yao, Appl. Phys. Lett. **84**, 4562 (2004).
[11] Y. Wang, X. L. Du, Z. X. Mei, Z. Q. Zeng, M. J. Ying, H. T. Yuan, J. F. Jia, Q. K. Xue, and Z. Zhang, Appl. Phys. Lett. **87**, 051901 (2005).
[12] S. K. Hong, T. Hananda, Y. Chen, H. J. Ko, T. Yao, D. Imai, K. Araki, and M. Shinohara, Appl. Surf. Sci. **190**, 491 (2002).
[13] The RHEED pattern became streaky on impinging O plasma onto a CrN surface, while the reciprocal spacing was changed from the value for CrN to that for Cr_2O_3.
[14] H. C. Gatos, J. Appl. Phys. **32**, 1232 (1961).
[15] A. N. Mariano and R. E. Hanneman, J. Appl. Phys. **34**, 384 (1963).
[16] D. Zhuang and J. H. Edgar, Mater. Sci. Eng., R. **48**, 1 (2005).
[17] J. L. Rouviere, J. L. Weyher, M. S. Eggebert, and S. Porowski, Appl. Phys. Lett. **73**, 668 (1998).
[18] A. R. Smith, R. M. Feenstra, D. W. Greve, M.-S. Shin, M. Skowronski, J. Neugebauer, and J. E. Northrup, Appl. Phys. Lett. **72**, 2114 (1998).
[19] X. Wang, Y. Tomita, O. H. Roh, M. Ohsugi, S. B. Che, T. Ishtani, and A. Yoshikawa, Appl. Phys. Lett. **86**, 011921 (2005).
[20] H. Tampo, P. Fons, A. Yamada, K. K. Kim, H. Shibata, K. Matsubara, S. Niki, H. Yoshikawa, and H. Kanie, Appl. Phys. Lett. **87**, 141904 (2005).
[21] T. Minegishi, J. H. Yoo, H. Suzuki, Z. Vashaei, K. Inaba, K. S. Shim, and T. Yao, J. Vac. Sci. Technol. B **23**, 1286 (2005).
[22] H. Kato, M. Sano, K. Miyamoto, and T. Yao, J. Cryst. Growth **265**, 375 (2004).
[23] X. G. Wang and J. R. Smith, Phys. Rev. B **68**, 201402 (2003).
[24] Z. X. Mei, Y. Wang, X. L. Du, M. J. Ying, Z. Q. Zeng, H. Zheng, J. F. Jia, Q. K. Xue, and Z. Zhang, J. Appl. Phys. **96**, 7108 (2004).
[25] P. Michel and Ch. Jardin, Surf. Sci. **36**, 478 (1973).